Available online www.jocpr.com

Journal of Chemical and Pharmaceutical Research, 2014, 6(2):532-540

Research Article

ISSN : 0975-7384
CODEN(USA) : JCPRC5

Nitrogen oxide decomposition improved by CH_2O additive through pulse streamer discharge

Xiaojun Wang, Lianshui Zhang*, Weidong Lai and Xueliang Cheng

College of Physics Science and Technology, Hebei University, Wusidonglu, Baoding, Hebei Province, P. R. China

---

ABSTRACT

Nitrogen oxide (NO) exhaust gas has deteriorated the natural air environment. In this article, the pulse streamer discharge technique is applied to remove such gas. Emission spectra indicate that NO has been decomposed into O and N by electron collision, and further productions such as N_2 and NO_2 are also found in the discharge. A zero-dimensional reaction model is established, and reveals that most of NO has been transformed into NO_2 and N_2, with N and O as essential intermediate radicals. In order to improve the NO removing process, the formaldehyde (CH_2O) at 1% concentration ratio is added, and the NO removal efficiency has been obviously heightened. NO molecules are transformed into other forms with NO_2, N_2, CO as major productions and a little of H_2O also appeared. The modified main reaction kinetics is evaluated. Furthermore, more CH_2O additive have arose out higher NO removal efficiency, due to more radicals of HCO and HNO produced from CH_2O for further accelerating the NO removal reactions. CH_2O additive is beneficial for NO pollutant gas remediation through the pulse streamer discharge technique.

Keywords: NO, CH_2O additive, pulse discharge, streamer discharge, non-thermal plasma

---

INTRODUCTION

Nitrogen oxide (NO) emission from automobiles, power plants or factory exhausts has induced serious environmental problems together with SO_2, such as the acid rain deposition [1-2]. Its oxidized species of NO_2 can further produce the photochemical smog [3]. Such pollution has deteriorated the natural air environment in Asia especially in China [4]. Many methods have been practiced to treat NO exhaust gas. The direct combustion is efficient though it should be applied at very high temperature [5]. Nowadays, the catalyzing reduction on NO_x has been focused on. But such technique usually requires temperature higher than 100 ℃ [6-7]. The two techniques are not suitable for NO removal at compact space in automobiles or other civil machines. Non-thermal plasma technique is a candidate for such purpose, and the inputted electrical energy can be efficiently utilized for generating high energy electrons rather than heating the exhaust gas [8]. NO molecules are decomposed after colliding by electrons, and chemical-physical reactions are further carried out between the radicals [9]. There have many reactions embedded, and the emission spectra, FT-IR detection and so on have been applied for monitoring the macroscopic irradiation from the discharged gas [10-11]. Concentration variance of productions in discharge is usually obtained through time-resolved spectra [12].

Investigations imply that the N or O atoms decomposed from NO can further deoxidize NO into N_2 or oxidize NO into NO_2 as well as other higher order nitrogen oxides (N_xO_y) [13-14]. The injected electrical energy is essential for such dissociation of NO. But question must be put forwards to find adequate methods for removing NO with higher efficiency at lower energy consumption. One way is to modify the discharging technique. For example, the radio-frequency (RF) discharge technique can resonantly accumulate lower electrical field into very high energy [15]. The other way is the additive gases for adjusting the reaction directions. The CH_4, NH_3 or even H_2O etc. are found effective when mixed with NO at suitable concentration ratio. The fractures of additive gases or even

themselves can react with NO or the decomposed components such as N or O [16-17].

The formaldehyde (CH_2O) is an important but poisonous reactant. Its additive effect on NO removal in discharge technique has drawn few attentions. In this article, the emission spectra from NO discharging plasma is detected and evaluated. Then a zero-dimensional model is established. The removal process of pure NO or NO mixed with a little of CH_2O additive gas is kinetically monitored. In Sec. 2, the discharging system is introduced. In Sec. 3, the experimentally detected emission spectra and the numerically simulated concentration variance of the productions are discussed. Conclusion is finally followed.

EXPERIMENTAL SECTION

The emission spectra have been experimentally detected from discharge, and a zero-dimensional reaction model is established and numerically processed.

2.1 Pulse streamer discharge system for NO removal

The NO and other gas are delivered into the glass tube from gas cylinders, and their concentration ratio is controlled by the gas valves. The discharge is taking place between two pointed tungsten needles in the glass tube initiated by pulse high voltage. Bright filament is observed between the needles, and its irradiation is collected and recorded by optical system consisted by the lens, monochromator and Boxcar. The signals are further analyzed to investigate the NO decomposing process.

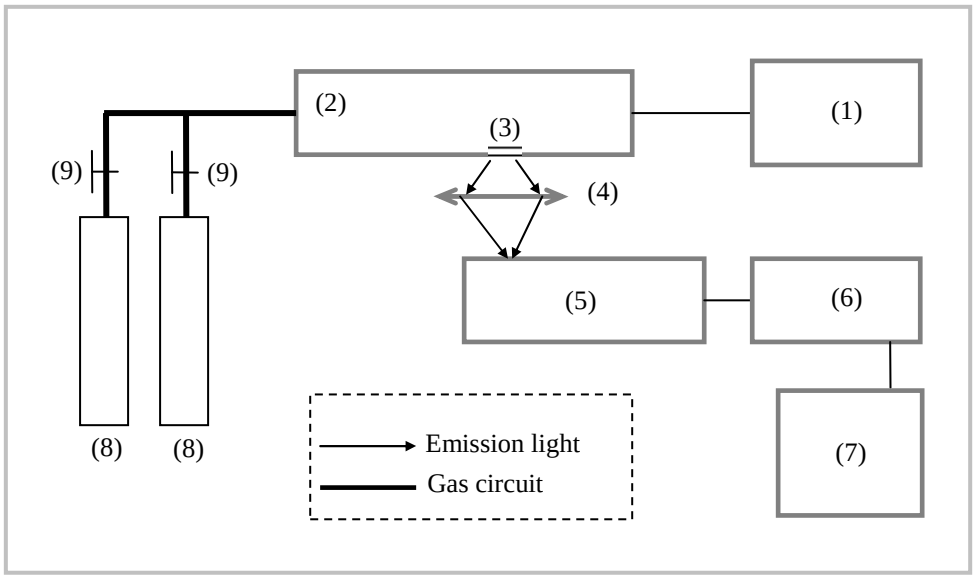

Fig. 1 The diagram of pulse streamer discharge system for NO removal

(1) Power supply, (2) glass discharging tube, (3) quartz window, (4) lens, (5) monochromator (ARC, AM-566), (6) Boxcar (SRS 280/255), (7) computer, (8) gas cylinders, (9) gas valves

The pulse discharge is carried out at room temperature, and pressure in the glass discharging tube is set to 1 atm. The recorded spectra signal is 0.1 nm resolved. The voltage is loaded at 4.8 kV with pulse width of 50 ns.

2.2 Numerical simulating method

There would have many chemical-physical reactions during and after the discharge. The reactions can be numerically monitored.

For a reaction, it can be defined as

$$A + B \rightarrow C \quad \textbf{(1)}$$

The concentration variance of A, B and C can be mathematically denoted by differential equations as

$$\frac{d[A]}{dt} = -k[A][B]$$

$$\frac{d[B]}{dt} = -k[A][B]$$
$$\frac{d[C]}{dt} = +k[A][B] \quad \textbf{(2)}$$

In which, *k* is the reaction rate coefficient.

Such differential equations can form an equation system when several reactions are considered. It should be noticed that no spatial components are appeared in Eq.(2), and the equations are only related to time variance. The equation system is zero-dimensional, and can be solved by *Runge-Kutta* method [18].

RESULTS AND DISCUSSION

3.1 Emission spectra diagnosis on the pulse streamer discharged NO gas

The emission spectra in Fig. 2a are utilized to determine the production categories in the discharge. There has a sequence of emission peaks appeared, and the highest emission is at 777.1 nm. When locally amplifying the spectra, such as the wavelength range from 220 to 290 nm in Fig. 2b, the emissions are not sharp lines but profiles with definite widths.

Such width of emissions is derived from two factors. One is the *instrumental broadening* from the monochromator, and the other is that there have emissions irradiated from molecules which possesses continuous energy band structure. For example, the emissions in the UV range are obviously corresponding to molecules with semi-continuous energy bands, and the emission at 777.1 nm is probably sourced from the atom irradiation due to its sharpness.

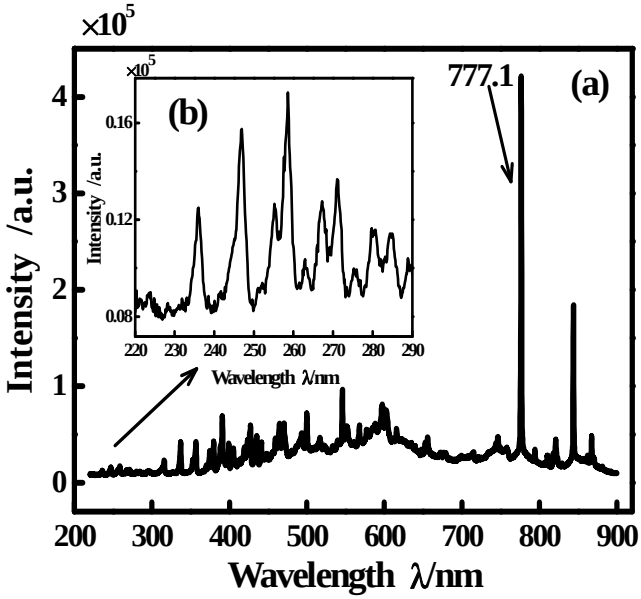

Fig. 2 (a) The emission spectra of NO in the pulse streamer discharge at the wavelength range from 220 to 900 nm, and (b) the locally amplified spectra at the UV band

Such emissions and the corresponding species categories have been vastly investigated during the pervious century, and can be conveniently evaluated. After inquiring the *NIST database* [19], the emissions are classified in Table 1. New productions such as molecules of N_2 and NO_2 or atoms of N and O have been discriminated out. It means that a part of NO molecules have been decomposed and further recombined into new productions.

Tab. 1. The evaluated species categories and the corresponding irradiation paths

Emission bands /nm	Categories	Transition paths
236.3 - 294.4	NO	$A^2\Sigma \rightarrow X^2\Pi$
297.7 - 470.6	N_2, N_2^+	$C^3\Pi_u \rightarrow B^3\Pi_g$
494.0 - 673.6	NO_2	$A^2B_1 \rightarrow X^2A_1$
746.4, 821.4, 867.6	N	$2s^22p^2(^3P)3p \rightarrow 2s^22p^2(^3P)3s$
777.1, 844.2	O	$2s^22p^3(^4S°)3p \rightarrow 2s^22p^3(^4S°)3s$

The reactions in discharge must include the electron impact dissociation on NO, and other reaction routes should be further analyzed.

3.2 Numerical simulation of NO removal reactions through pulse streamer discharge

The reactions embedded in the discharge are evaluated. The first one is the decomposition of NO collided by electrons. Then the produced atoms of N and O are further reacted with NO due to the high concentration of NO molecules, which means higher collision probabilities between NO and N or O. Finally, there also have minor reactions between N or O themselves. Such reactions are outlined in Table 2, with the corresponding rate coefficients present. The reaction rate coefficients have been inquired from *NIST database* except that of the direct electron impact decomposition of NO, which is calculated in this article based on the collision cross sections.

There have eight reactions outlined in Table 2.

Tab. 2 Reactions and corresponding rate coefficients of discharged NO gas [20]

R.	Reactions	k /cm^3s^{-1}
R1	$e^*+NO \rightarrow N+O+e$	8.50×10^{-10}
R2	$NO+N \rightarrow N_2+O$	3.22×10^{-11}
R3	$NO+O \rightarrow NO_2$	3.01×10^{-11}
R4	$NO+O \rightarrow O_2+N$	3.68×10^{-13}
R5	$N+N \rightarrow N_2$	1.25×10^{-32}
R6	$O+N \rightarrow NO$	3.03×10^{-32}
R7	$O+O+N_2 \rightarrow O_2+N_2$	1.10×10^{-33} [a]
R8	$O_2+NO+NO \rightarrow NO_2+NO_2$	3.67×10^{-39} [a]

[a] *The unit is cm^6s^{-1} for the three order reactions.*

Consequently, the reactions are graphically schemed in order to elucidate the main reaction routes. In Fig. 3, the N_2, O_2 as well as NO_2 are expected as main productions. The N_2 and O_2 are benign, and the NO_2 also can be removed conveniently by alkali scrub. In the scheme, N and O have played essential roles.

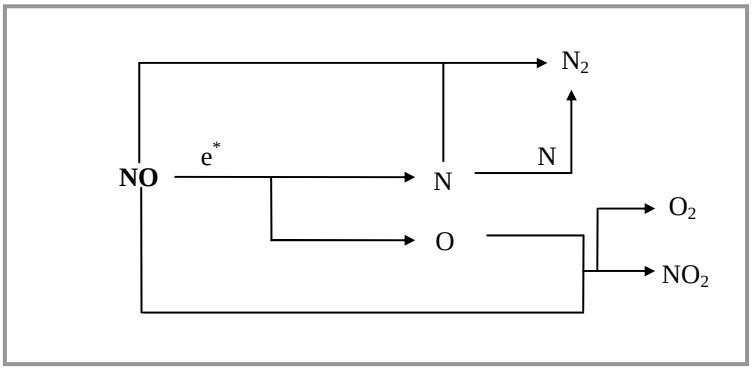

Fig. 3 The reaction routes of pure NO during and after pulse streamer discharge

The simulating results are shown in Fig. 4. During discharge, a part of NO has been removed and NO concentration is monotonically decreased. The removal efficiency (η) is achieved to about 4.1198%. After discharge, the production concentrations are not distinctly varied.

Such phenomenon is ascribed that the N and O as the decomposed productions of NO are decided by electron collision, and their generations have been restricted by the discharge pulse process. After discharge, the N and O have been fast consumed out in Fig. 4b.

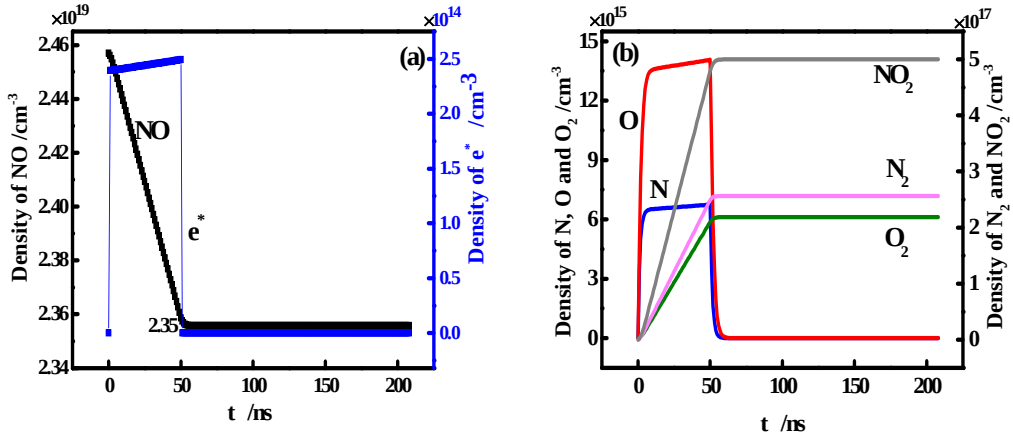

Fig. 4 Time resolved concentration evolution of (a) NO and electron, and (b) N, O, O_2 (corresponding to the left axis), and N_2, NO_2 (corresponding to right axis)

Tab. 3 Reactions related to NO and the additive gas of CH_2O, and their corresponding rate coefficients [20]

R.	Reactions	k /cm^3s^{-1}
R1	$NO+CH_2O \rightarrow HCO+HNO$	2.83×10^{-13}
R2	$NO+HCO \rightarrow CO+HNO$	1.35×10^{-11}
R3	$NO+HNO \rightarrow OH+N_2O$	7.14×10^{-13}
R4	$HCO+HNO \rightarrow CH_2O+NO$	8.19×10^{-13}
R5	$HCO+O \rightarrow CO+OH$	5.00×10^{-11}
R6	$HCO+O \rightarrow CO_2+H$	5.00×10^{-11}
R7	$HCO+NO_2 \rightarrow CO+HNO_2$	2.95×10^{-20}
R8	$HCO+NO_2 \rightarrow CO_2+NO+H$	1.93×10^{-11}
R9	$HNO+O \rightarrow NO_2+H$	2.01×10^{-14}
R10	$HNO+O \rightarrow O_2+NH$	1.88×10^{-16}
R11	$HNO+O \rightarrow OH+NO$	5.99×10^{-11}
R12	$NO+NH \rightarrow OH+N_2$	1.41×10^{-12}
R13	$NO+NH \rightarrow N_2O+H$	5.89×10^{-12}
R14	$NO+H \rightarrow NH+O$	6.10×10^{-13}
R15	$NO+H \rightarrow OH+N$	2.48×10^{-12}
R16	$NH+N \rightarrow N_2+H$	8.18×10^{-11}
R17	$NH+H \rightarrow H_2+N$	1.69×10^{-11}
R18	$NH+H \rightarrow H+H+N$	9.82×10^{-13}
R19	$HNO+HNO \rightarrow H_2O+N_2O$	1.02×10^{-15}
R20	$HNO+H \rightarrow NH_2+O$	2.39×10^{-11}
R21	$HNO+NH_2 \rightarrow NH_3+NO$	7.30×10^{-11}
R22	$HNO+H \rightarrow OH+NH$	9.71×10^{-11}
R23	$HNO+H \rightarrow H_2+NO$	2.72×10^{-11}
R24	$HNO+NO_2 \rightarrow HNO_2+NO$	8.19×10^{-13}
R25	$HNO+OH \rightarrow H_2O+NO$	5.00×10^{-11}
R26	$HNO_2+O \rightarrow OH+NO_2$	1.10×10^{-11}
R27	$HNO_2+H \rightarrow OH+HNO$	8.64×10^{-11}
R28	$HNO_2+NO_2 \rightarrow HNO_3+NO$	1.00×10^{-22}
R29	$HNO_2+HNO_2 \rightarrow H_2O+NO+NO_2$	9.48×10^{-19}
R30	$HNO_2+OH \rightarrow H_2O+NO_2$	6.00×10^{-12}
R31	$NO+OH \rightarrow HNO_2$	4.57×10^{-34}
R32	$N_2O+H \rightarrow OH+N_2$	3.50×10^{-11}
R33	$NO+N_2O \rightarrow N_2+NO_2$	3.36×10^{-12}
R34	$NO+NH_2 \rightarrow N_2+H_2O$	2.14×10^{-13}
R35	$NH_3+NO \rightarrow NH_2+HNO$	1.45×10^{-13}
R36	$NH_3+O \rightarrow OH+NH_2$	7.68×10^{-12}
R37	$NH_3+NH \rightarrow NH_2+NH_2$	3.55×10^{-11}
R38	$NH_3+H \rightarrow H_2+NH_2$	3.03×10^{-11}
R39	$NH_3+NO_2 \rightarrow HNO_2+NH_2$	3.26×10^{-14}
R40	$HNO_2+NH_2 \rightarrow NH_3+NO_2$	8.30×10^{-14}

The O and N maximal concentration is at the magnitude order of 10^{15} and 10^{16} cm^{-3}, which are lower than that of N_2 and NO_2 at 10^{17} cm^{-3}. It means that the O and N have been uninterruptedly reacted with NO to accumulate NO_2 and N_2, and the NO_2 and N_2 have no further consuming routes.

Additionally, it should be noticed that there also have some O_2 molecules generated, though its concentration at magnitude order of 10^{15} cm^{-3} is remarkably lower than that NO_2 and N_2. The oxidization on NO by O is obviously faster than the recombination process between two O atoms to form O_2.

3.3 Effect of CH_2O additive on NO decomposition through the pulse streamer discharge

The formaldehyde (CH_2O) is also a kind of pollutant gas and poisonous to human beings, even though it is consumed at very large quantities in factories. In given cases, the CH_2O can be naturally or artificially mixed with NO gas. Its effect on NO decomposition through the pulse discharge technique is considered in this article. The CH_2O concentration ratio to NO is 1%.

The reactions related to CH_2O and NO are outlined in Table 3, with the corresponding rate coefficients followed.

After CH_2O added, simulation indicates that the concentration variances of O, N and O_2 are not distinctively affected in Fig. 5a, but the N_2 as well as NO_2 have been remarkably influenced. The NO removal extent has been improved in Fig. 5b.

Since the improvement is mainly achieved after discharge at a relatively slow trend, it means that the electron impact dissociation on NO has played the essential role during discharge, and the CH_2O effect is slowly displayed after discharge. Such a phenomenon is ascribed that the CH_2O is reacted with NO at rate coefficient of 2.83×10^{-13} cm^3s^{-1}, which is 10^{-3} order lower than the electron impact dissociation at 8.50×10^{-10} cm^3s^{-1}. And the CH_2O molecules do not influence the electron impacting kinetics in the model due to its low concentration ratio of 1%.

The NO removal efficiency has been heightened from 4.1198% to 7.1589%, or in other words more 7.4671×10^{17} cm^{-3} NO molecules have been reduced. N and O elements in the more reduced NO molecules have been transformed into other forms assisted by CH_2O.

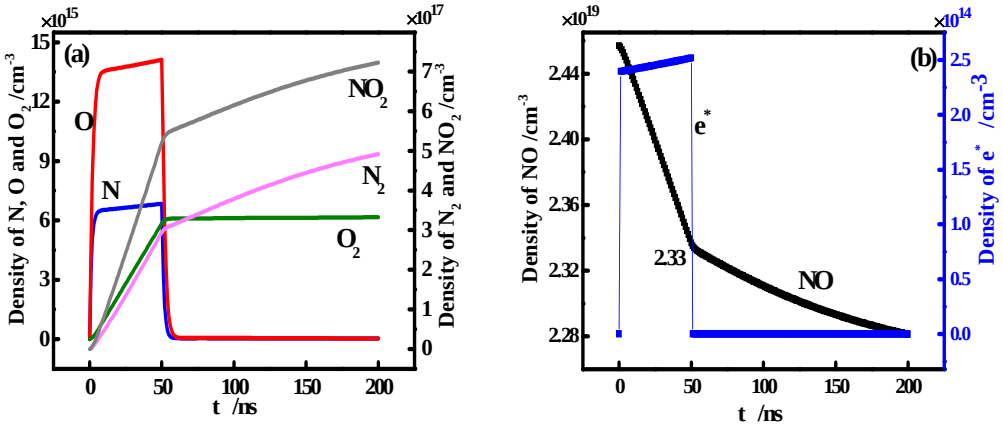

Fig. 5 Time resolved concentration evolution of (a) N, O, O_2 (corresponding to left axis), and N_2, NO_2 (corresponding to right axis), and (b) NO and electrons

It is obvious that most of the N elements in the further reduced NO have transformed into N_2 and NO_2 in Fig. 5a. For the more reduced O elements, the final produced NO_2 also hold the major part.

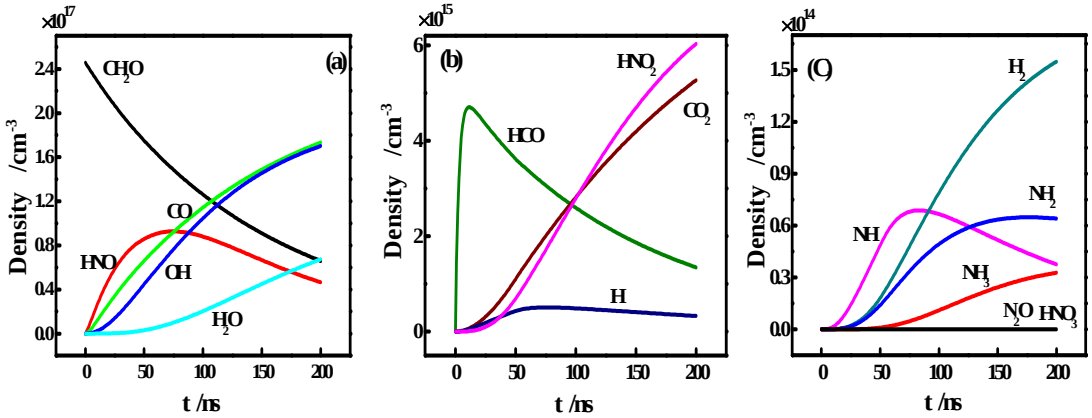

Fig. 6 Time resolved concentration evolution of (a) the CH_2O, HNO, CO, OH, H_2O, (b) the HCO, HNO_2, CO_2, H, and (c) the H_2, NH_2, NH, NH_3, N_2O as well as HNO_3

In order to discriminate the NO removal kinetics assisted by CH_2O, concentration variances of the other productions

containing C, H and O as well as the residual N elements are present in Fig. 6. There have CO and H_2O finally generated as the major productions. The other productions are only accumulated to relatively low concentrations in Fig. 6b and c, such as HNO_2, CO_2, H_2, NH_3, N_2O as well as HNO_3.

For the radicals, the final concentrations of H, NH and NH_2 are ignorable. But the OH radicals have been accumulated to high concentration at 10^{17} cm^{-3} magnitude order. It also should be noticed that most of the CH_2O, about 73.2052%, have simultaneously been removed, and the HNO and HCO radicals sourced from CH_2O have been nearly consumed out after the simulation.

The main reaction routes of NO removal assisted by CH_2O during and after discharge are clarified from the above time-resolved analysis, and diagrammatically schemed in Fig. 7. Other reactions are minor and have been ignored.

The radicals of HNO and HCO sourced from the reaction between NO and CH_2O are played the essential roles, and the HNO is more important than HCO in the kinetic scheme. Another key radical is OH, and it has acted as essential intermediate reactant to remediate the poisonous pollutant HNO_2 into benign productions of H_2O and easy-scrubbed component of NO_2. For the C element in CH_2O, it has been transformed into CO and a small part of CO_2.

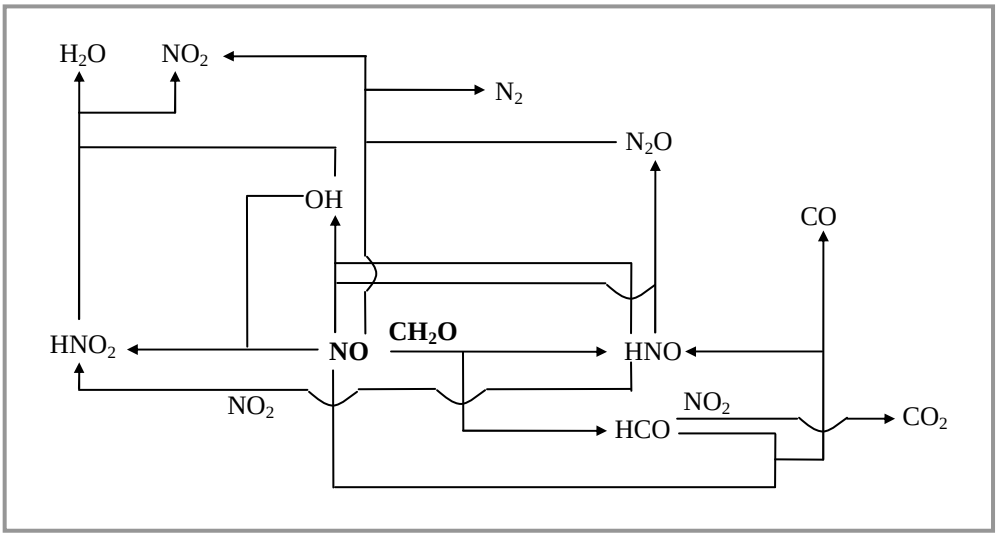

Fig. 7 Main reaction routes for removing NO assisted by CH_2O additive gas during and after pulse streamer discharge

It should be noticed that the spatial diffusion of all the molecules, atoms and radicals in the reaction scheme have been ignored in such zero-dimensional simulating model.

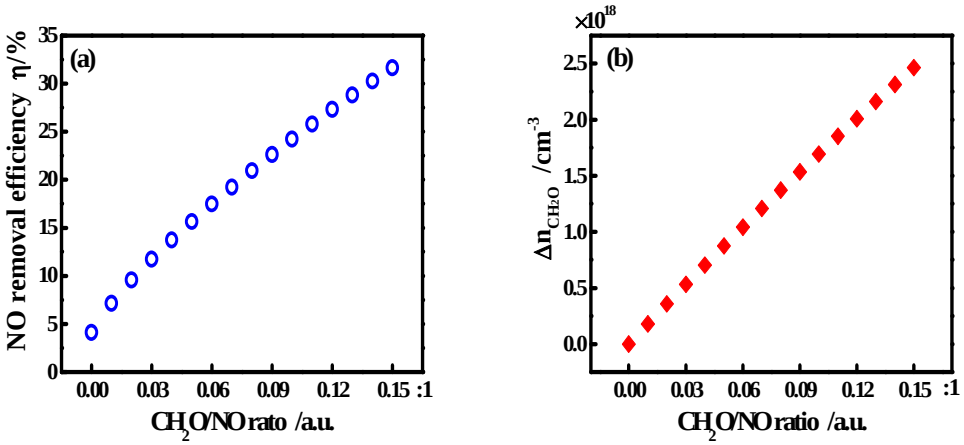

Fig. 8 Under different CH_2O/NO concentration ratio, (a) the NO removal efficiency, and (b) the CH_2O concentration variance (Δn_{CH2O}) after the simulation

The CH_2O molecules are slightly increased from the concentration ratio of 1% to 15%, and CH_2O concentration effect is present in Fig. 8a. NO removal efficiency (η) presents a monotonically increasing trend.

Such a phenomenon is ascribed to the reaction ruled by

$NO+CH_2O \rightarrow HCO+HNO \qquad k=2.83\times10^{-13}\ cm^3s^{-1}$ **(3)**

More CH_2O additive has heightened the consumption extent of NO, and more radicals of HNO and HCO have been produced for further accelerating the NO removal reactions schemed in Fig. 7.

Such deduction is verified in Fig. 8b that more CH_2O molecules have been consumed to participate into the reaction present in Eq.(3) and transformed into active radicals when CH_2O/NO ratio increased.

CONCLUSION

NO removal through pulse streamer discharge is applied in this article. Evaluation on the experimentally collected emission spectra implies the effective decomposition of NO by electron collision, and more physical-chemical reactions are embedded. Based on the numerical results derived from the established zero-dimensional model, the major productions during the discharge are revealed as NO_2 and N_2, which are sourced from the reactions of NO with radicals of O or N. The CH_2O additive has efficiently improved the NO removal kinetics mainly after discharge, due to the relatively low rate coefficient of the reaction between CH_2O and NO. The main NO removal routes assisted by CH_2O are determined by the intermediate radicals such as HCO, HNO and OH. The productions are including the benign species of N_2, H_2O, or easy-scrubbed species as NO_2 and CO. Higher ratio of CH_2O additive have supplied more HCO and HNO radicals, and further accelerated the NO removal.

NO removal kinetics have been adjusted by a little of CH_2O additive, and the CH_2O itself as a kind of pollutant ingredient is also simultaneously remediated. The pulse streamer discharge technique is beneficial for high-efficiently reducing NO when adequate additive gas is mixed.

Acknowledgments
This work was financially supported by National Nature Science Foundation of China No. 10875036, and the Nature Science Foundation of Hebei Province No. A2007000131, A2010000177.

REFERENCES

[1] XJ Liu; L Duan; JM Mo; EZ Du; JL Shen; XK Lu; Y Zhang; XB Zhou; C He; FS Zhang. *Environ. Pollut.*, **2011**, 159(10), 2251-2264.
[2] VM Priyanka; D Sirisha; N Gandhi. *J. Chem. Pharm. Res.*, **2012**, 4(3), 1768-1771.
[3] S Gnanasekaran; K Subramani; AT Ansari. *J. Chem. Pharm. Res.*, **2010**, 2(5), 153-160.
[4] ZY Meng; B Xu; T Wang; XY Zhang; XL Yu; SF Wang; WL Lin; YZ Chen; YA Jiang; XQ An. *Atmos. Environ.*, **2010**, 44(21), 2625-2631.
[5] D Kühnemuth; F Normann; K Andersson; F Johnsson; B Leckner. *Energ. Fuel.*, **2011**, 25(2), 624-631.
[6] S Chauhan. *J. Chem. Pharm. Res.*, **2010**, 2(4), 602-611.
[7] S Chauhan. *J. Chem. Pharm. Res.*, **2010**, 2(4), 489-495.
[8] K Skalska; JS Miller; S Ledakowicz. *Sci. Total Environ.*, **2010**, 408(19), 3976-3989.
[9] A Mizuno; R Shimizu; A Chakrabarti; L Dascalescu; S Furuta. *IEEE T. Ind. Appl.*, **1995**, 31(5), 957-962.
[10] K Shimizu; T Oda. *Sci. Technol. Adv. Mat.*, **2001**, 2(3), 577-585.
[11] M Baeva; H Gier; A Pott; J Uhlenbusch; J Höschele; J Steinwandel. *Plasma Sources Sci. Technol.*, **2002**, 11(1), 1-9.
[12] S Welzel; O Guaitella; C Lazzaroni; CD Pintassilgo; A Rousseau; J Röpcke. *Plasma Sources Sci. Technol.*, **2011**, 20(1), 015020.
[13] GB Zhao; X Hu; MD Argyle; M Radosz. *Ind. Eng. Chem. Res.*, **2004**, 43(17), 5077-5088.
[14] TQ Vinh; S Watanabe; T Furuhata; M Arai. *J. Mech. Sci. Technol.*, **2012**, 26(6), 1921-1928.
[15] T Yumii; T Yoshida; K Doi; N Kimura; S Hamaguchi. *J. Phys. D Appl. Phys.*, **2013**, 46(13), 135202.
[16] M Schmidt; R Basne; R Brandenburg. *Plasma Chem. Plasma P.*, **2013**, 33(1), 323-335.
[17] FJCM Beckers; WFLM Hoeben; AJM Pemen; EJM van Heesch. *J. Phys. D Appl. Phys.*, **2013**, 46(29), 295201.
[18] J Butcher. Numerical methods for ordinary differential equations, John Wiley & Sons, New York, **2003**; 123-185.
[19] A Kramida; Y Ralchenko; J Reader; NIST ASD Team. NIST Atomic Spectra Database, Version 5.1, National Institute of Standards and Technology, Gaithersburg, Maryland, **2013**; URL: http://physics.nist.gov/asd.
[20] JA Manion; RE Huie; RD Levin; DR Burgess Jr.; VL Orkin; W Tsang; WS McGivern; JW Hudgens; VD Knyazev; DB Atkinson; E Chai; AM Tereza; CY Lin; TC Allison; WG. Mallard; F Westley; JT Herron; RF Hampson; DH Frizzell. NIST Chemical Kinetics Database, NIST Standard Reference Database 17, Version 7.0 (Web Version),

Release 1.4.3, National Institute of Standards and Technology, Gaithersburg, Maryland, **2008**; URL: http://kinetics.nist.gov/.